Identifying Weak Areas of Urban Land Use Carbon Metabolism in High-Density City

Zongliang Lu[ab*], Xiaobing Zhang[b], Yilun Liu[c], Liying Yang[d], Lu Yi[d]
[a] *Key Laboratory of Natural Resources Monitoring in Tropical and Subtropical Area of South China, Guangzhou, China;*
[b] *School of Public Administration, Guangdong University of Finance & Economics, Guangzhou, China;*
[c] *School of Public Administration, South China Agricultural University, Guangzhou, China;*
[d] *Guangdong Provincial Institute of Land Surveying and Planning, Guangzhou, China*
zonglianglu@outlook.com

Abstract
For high-density cities, it is necessary for city managers to achieve precise regulation of carbon emissions and sequestration. For reference, taking Dongguan as example, this study proposed a complex framework to identify weak areas of urban land use carbon metabolism in high-density city. On the basic of defining the urban land use carbon metabolism units, LEAP, Markove-PLUS, and LANDIS model were applied to spatialize land use carbon emissions and carbon sequestration. Finally, the weak areas of urban land use carbon metabolism were clearly indicated through overlapping the spatial pattern of land use carbon emissions and sequestration. Accordingly, carbon emissions limit regions can be delimited, and its carbon emissions are recommended to be metabolize through connecting the limit regions to green spaces with various ecological corridors. The results will serve as a foundation to plan and control carbon emissions in high-density cities that are similar to Dongguan in international communities.

Key words: Weak areas; urban land use; carbon metabolism; high-density city

1. Introduction

Although urban areas only make up 2% of the world's surface area, they are responsible for around 75% of the world's carbon dioxide emissions [1]. Dongguan, a manufacturing city in the east of China's Pearl River Delta, it has undergone rapid industrialization in the past 30 years. Large tracts of vegetated surfaces were replaced with built-up land to support the growth of manufacturing. This highly unbalanced carbon emissions and sequestration caused variations in carbon metabolism among different land use types and geographic areas. Due to the barrier of buildings, carbon metabolism in high-density cities may not have obvious spatial correlation and spillover effect [2]. In order for city administrators to implement targeted measures to control carbon catabolism in high-density cities, it is necessary to develop specific ideas to identify weak areas of urban carbon metabolism. In an effort to gauge the degree of carbon emissions from cities, the urban carbon metabolism (UCM) concept was applied [3]. Researchers have paid close attention to this theory, which was first proposed by Baccini [4]. Recently, it was found it crucial to quantify urban carbon emissions and sequestration of both natural and anthropogenic components [5].

Ideas for accounting UCM can be divided into two categories [6]. The first category is to build top-down models that extend to the energy and climate systems based on traditional economic models [7]. Although top-down models were suitable for exploring the path of carbon metabolism under macroeconomic policies, climate policies and energy policies, they are insufficient to predict regional carbon metabolism and difficult to explain the related processes such as economic refinement, technological progress and regional linkage [8]. Another category is to build bottom-up models which evolves to the economic and environmental modules based on energy economic model [9]. Bottom-up models are more suitable for technical decision-making of energy supply and demand forecast. Among, Long-range Energy Alternatives Planning System model (LEAP) was widely employed to analyze the energy consumption and carbon emissions [10]. Nonetheless, in quantifying process, less consideration was given to the attribute difference of natural environment, which leads to insufficient spatial analysis of UCM [11]. Thus, the quantifying results may be too rough to be applicable for identifying weak areas of UCM at urban scale. In order to present spatial processes, UCM therefore should concentrate on carbon flows caused by land use cover & change (LUCC) between the different components of the urban land system [13]. To describe the relationship between LUCC and UCM, urban land use carbon metabolism (ULUCM) was advanced [14]. Methods for accounting ULUCM included field surveys, the process method, and the remote-sensing method [15]. In addition, scholars have combined empirical data, remote-sensing data, and geographic information to give better spatial expression of ULUCM. Traditional prediction models, such as CA and Markov model, were widely applied in simulating land use carbon emissions and sequestration at urban scale [16]. These studies are benefit for describing the

pattern of land-use changes, enabling policymakers to create site-specific regulations that will limit land-use change in ways that boost carbon sequestration or lower carbon emissions. Current spatial pattern of ULUCM as well as its weak areas can be accurately distinguished.

However, LUCC is a dynamic change process, the spatial pattern as well as weak areas of ULUCM will change accordingly. In the process of setting scenario parameters and accounting land use carbon coefficient, more attention was paid to historical law of land use change, less consideration was given to the demand of energy consumption require for socio-economic and industrial development. That is, results of carbon emissions prediction of energy consumption at regional scale may not consistent with the simulated pattern of land use carbon emissions at urban scale. If so, it will not be accurate enough to simulate the future spatial pattern of ULUCM. In order to implement targeted measures to reduce carbon emissions and increase carbon sequestration for high-density cities, UCM research should shift the focus to identify the weak areas of ULUCM that are consistent with the future demand of energy consumption required for socio-economic and industrial development.

Therefore, this paper integrated the ideas of scenario simulation of carbon emissions from energy consumption, simulation of land use carbon emissions, and estimation of land use carbon sequestration, to build special model that can identify the weak areas of ULUCM in consistent of future possible energy consumption. As shown in Fig. 1, the following aspects were addressed: 1) To predict the total carbon emissions from energy consumption of urban area under various carbon emissions reduction measures according to current situation of socio-economic development and industrialization with LEAP model; 2) To map the predict total carbon emissions on the future land use pattern to simulate the future land use carbon emissions pattern with Markov-Plus model; 3) To simulate the spatial pattern of future land use carbon sequestration according to the distribution of current urban green space and plant growth situation with LANDIS model; 4) To overlay the spatial pattern of land use carbon emissions and sequestration for the identification of ULUCM weak areas.

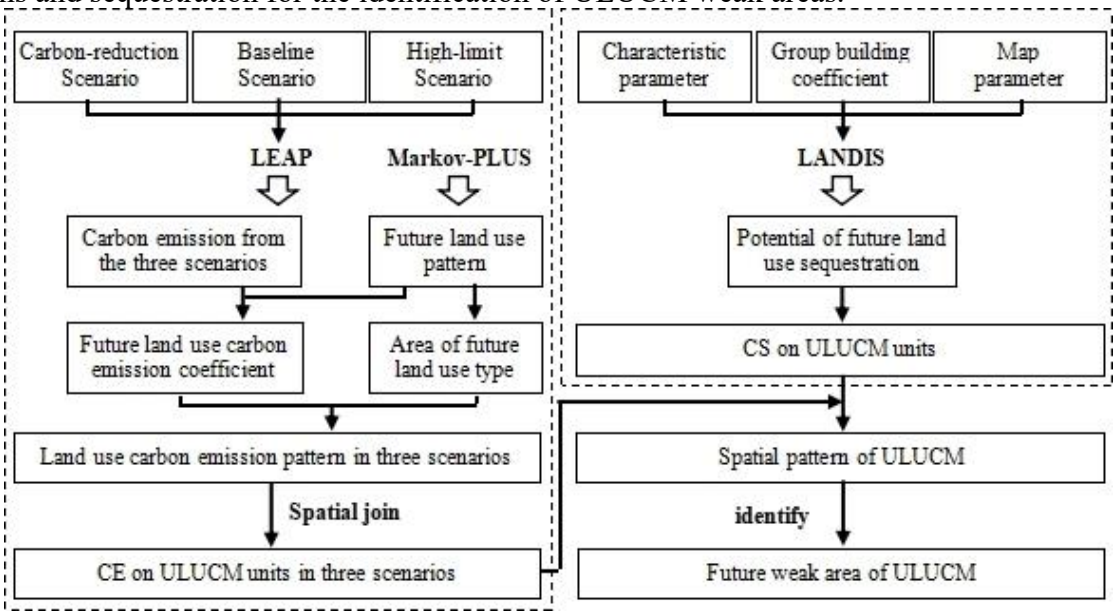

Figure 1. The Research Roadmap

2. Material and data sources

2.1. Study area

Dongguan, which located in the east of Pearl River delta Economic Zone, Guangdong Province, China (Fig.2). It is a high-density city which covers approximately 246,011.53 ha, 48.37% of which is built-up land. It contains six sub economic zones. Many ecological lands were turned into built-up areas as a result of industrialization, which dramatically increased the urban greenhouse effect and created a significant imbalance in UCM. Therefore, Dongguan is a typical city to study the coupling of macro prediction of energy consumption and micro-optimization of ULUCM pattern.

Considering that relevant policies need to be implemented by administrative districts, the administrative area of 672 village/block was set as ULUCM units.

2.2. Data Resources and Processing

This paper takes 2020 as the base year and 2030 as the target year. Data and parameters include energy consumption intensity data, tree species parameters, terrain elevation, etc. It is derived from the

Guangdong Implementation Plan of Near Zero carbon Emission Zone Demonstration Project, the Guangdong 14th Five-Year Energy Plan, the Dongguan National Economic and Social Development 14th Five-Year Plan and 2035 Vision Goals Outline, the Dongguan Energy 14th Five-Year Plan, the Dongguan Ecological Environment 14th Five-Year Plan, and so on.

Land-use vector map and remote sensing image (1:2000) were provided by department of natural resources. Raster Data on population density was downloaded from Open Spatial Demographic Data and Research (https://www.worldpop.org/). Point-of-interest data was collected from Google Earth. Raster data for GDP was collected from Zhao (2017)'s research results. All pertinent data were merged into a geographic information system database using ESRI Corporation's ArcGIS v10.2 software [17]. Urban land-use categories were identified using vectors with open-street maps and points-of-interest, as well as classification and visual interpretation of remote sensing monitoring. In order to connect the land use type with the industry type in the LEAP model, land use types were divided into eight categories: agricultural & forest land, green space, industry land, architecture land, specially-designated land, traffic land, water area, and unutilized land.

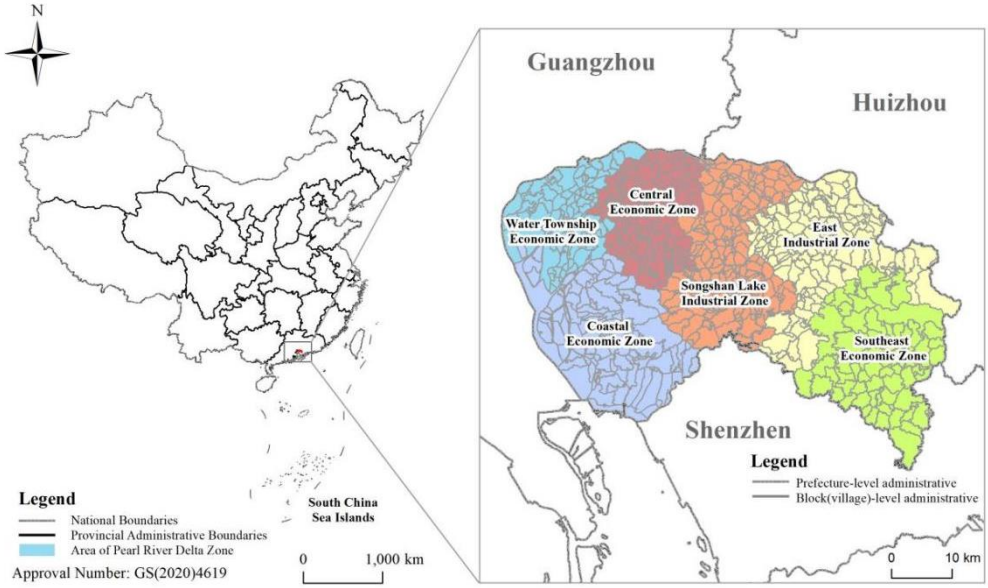

Figure.2 The location of the study area of Dongguan

3. Methodology

3.1. Simulating land use carbon emissions pattern

3.1.1 Predicting carbon emissions of energy consumption

As LEAP model has low requirements on data richness and differentiation, and can realize specific scenario simulation, it is very suitable for predicting carbon emissions of urban energy consumption. Scenario comparison is the core function of LEAP model. For comparison, three scenarios are defined as follows: 1) Baseline scenario, which continues current Dongguan's social and economic development, without considering the innovative application of new technologies and the implementation of new carbon emissions reduction policies. 2) Emission-reduction scenario, which refers to increasing urban emissions reduction measures based on baseline scenarios, such as increasing forestry carbon sinks. 3) High-limit scenario, which refers to the maximum increase of urban emissions reduction measures based on baseline scenario, such as promoting the large-scale and commercial application of carbon capture.

As Tab.1 shown, according to the parameter requirements of LEAP model, the model structure was set by retrieving statistical data. Based on baseline scenario, referring to local government's requirement and model decomposition, parameters of scenario indicators in three scenarios were set as Tab.2.

Table.1 LEAP Model Structure Setting

Department	Activity level	Energy intensity	Energy structure	Emission factor
Urban dweller	Permanent urban population * per capita housing floor area of urban residents	Energy consumption of residential area of urban units	Proportion of non-fossil energy (electricity, heat), proportion of fossil energy (coal, oil, gas, etc.)	CO_2, CH_4 (residential and agriculture, forestry, animal husbandry and fishery), N_2O default values
Rural dweller	Rural permanent population * per capita housing floor area of rural residents	Energy consumption per residential area in rural areas		

Business service construction	Area of commercial service land * average resident population density of commercial service land	Per capita consumption of fossil energy (coal, oil, gas, etc.) per unit land area of commercial service buildings	Proportion of non-fossil energy (electricity, heat)	CO_2, CH_4 (business and institutions), N_2O default values
Operational traffic	Permanent population * total passenger and freight turnover per capita	Per unit passenger-freight turnover energy consumption ratio of fossil energy (coal, oil, gas, etc.)		
Non-operational traffic	Permanent resident population * number of private cars per capita Annual energy consumption of private cars per unit of fossil energy	Annual electricity consumption per unit of new energy private cars Proportion of fossil energy private cars (diesel, gasoline)	Proportion of new energy private cars (electricity)	CO_2, CH_4 (energy and transportation), N_2O default values
Manufacturing industry	Industrial added value	Percentage of fossil energy consumption per unit of industrial added value (coal, oil, gas, etc.)	Proportion of non-fossil energy (electricity, heat)	CO_2, CH_4 (manufacturing and construction), N_2O default values
Construction industry	Value added of construction industry	Percentage of fossil energy consumption per unit value added of construction industry (coal, oil, gas, etc.)		
Agriculture and forestry production	Value added of the primary industry	Percentage of fossil energy consumption per unit value added of primary industry (coal, oil, gas, etc.)		CO_2, CH_4 (housing and agriculture, forestry, animal husbandry and fishery), N_2O default values
Forestry carbon sequestration	Land area * forest coverage rate, proportion of newly increased forest area, carbon sink per unit afforestation area		Proportion of original woodland area	Carbon sequestration per unit of forest area

Table.2 Parameters setting of scenario indicators

Scenario indicators		Parameters setting (by 2030)	Baseline	Emission-reduction	High-limit
Measure of baseline scenario		Current policy measures and technological level	√	√	√
Optimizing industrial structure		Increasing the proportion of the tertiary industry to 65%	-	√	√
Improving energy efficiency	Optimizing	Energy intensity in manufacturing and construction will be cut by 2% annually, and in agriculture and forestry by 4%. All urban residential buildings and rural residential-commercial buildings will be covered by the 50% and the 45% energy saving standard. By 2030, energy intensity of operational transportation will be reduced by 74% and that of private cars by 43.8%.	-	-	-
	Strengthening	Energy intensity in manufacturing and construction will be cut by an average of 4% annually, and in agriculture and forestry by 6%. Energy conservation standards for urban housing and rural residential and commercial buildings will be fully covered by 65% and 50 percent respectively. Energy intensity of operational transportation will be cut by 75%, and that of private cars by 46.4%.	-	√	√
Electrification	Optimizing	Annual consumption of non-fossil energy in manufacturing, construction, agriculture & forestry, urban housing, rural housing, commercial buildings, business transportation, and new energy vehicles will account for 60%, 40%, 60%, 70%, 80%, 85%, 30%, and 60%, respectively.	-	√	-
	Strengthening	Annual consumption of non-fossil energy in manufacturing, construction, agriculture-forestry, urban housing, rural housing, commercial buildings, business transportation, and new energy vehicles will account for 80%, 80%, 80%, 80%, 90%, 95%, 60%, and 80%, respectively.	-	-	√
Traffic	Optimizing	Operational traffic efficiency was optimized by 30%, and private cars in non-operational traffic was reduced by 30%	-	√	-
	Strengthening	Operational traffic efficiency was optimized by 45%, and private cars in non-operational traffic was reduced by 50%	-	-	√
Clean electricity	Optimizing	Non-fossil energy will account for 70% of electricity generation	-	√	-
	Strengthening	Non-fossil energy will account for 80% of electricity generation	-	-	√
commercialization of CCUS		CCUS will be commercialized on a large scale, and the capture rate of carbon emissions from industrial fossil energy will reach 8.5%	-	-	√
Forestry carbon sequestration		Forest coverage will reach 42%	-	√	-

3.1.2 Simulation of land use pattern

The future land use pattern can be simulated according to the following step:

Definition of Markov model. Markov model was selected as the simulation model to predict the number of land use types and simulate the land use pattern under the adaptive inertial cellular automata mechanism. The principle was:

$$S_{t+1} = P_{ij} \times S_t \quad (1)$$

where S_{t+1}, S_t represent the the land use status in period $t+1$ and t; P_{ij} is the probability that land use type i converted to land use type j.

Definition of PLUS model. The PLUS model was created using the Cellular Automata Model Based on Multitype Random Patch Seeds (CARS) and the Land Spread Analysis Strategy's (LEAS) rule mining framework. In this study, LEAS module was applied, which overlays the land use data of two periods to extract the cell with changing state from the late data of land use data, representing the change area of each land use type. On this fundamental level, it applied the double decision random forest classification algorithm to transform the mining of each land use type's conversion rules into a binary classification problem. The expression is:

$$P_{i,k(x)}^{\mathrm{d}} = \frac{\sum_{n=1}^{M} I(h_n(x) = d)}{M} \tag{2}$$

where $P_{i,k(x)}^{\mathrm{d}}$ is the development probability of land use type k in unit i. d has a value of 0 or 1. When d =1, represents that other land use types have changed into type k. When d=0, represents the transformation of land use type into other types except k. x refers to a vector made up of multiple driving factors. I refer to the indicator function of the decision tree. $h_n(x)$ refers to the prediction type of decision tree n of vector x. M is the total amount of decision trees.

Simulation of land use pattern. First, the expansion part of LUCC from 2010 to 2020 was extracted, and the significant factors that affected LUCC expansion were found out. Alternative factors include population, GDP, distance to road, distance to water area, slope, average annual temperature, and average annual precipitation. Second, based on LUCC's conversion rule, Dongguan's land use types and its amount in 2030 were predicted. Third, setting nature reserves as restricted areas, cellular automata with adaptive inertia mechanism in PLUS model was applied for spatial transformation allocation. Finally, the land use pattern in 2030 was simulated.

3.1.3 Simulation of land use carbon emissions pattern

The land use carbon emissions coefficient is the key to simulate land use carbon emissions pattern. Its relationship between carbon emissions of energy consumption and various land use types was set as follows:

$$CEEC_{\mathrm{ni}} = (A_1T_1 + A_2T_2 + \cdots + A_nT_n)_i \tag{3}$$

where $CEEC_{\mathrm{ni}}$ represent carbon emissions of energy consumption in scenario i that were predicted using LEAP; T_n refer to the total area of land use type n; A_n refer to the land use carbon emissions coefficient of land use type n, which were estimated by nonlinear fitting function on Matlab platform.

We multiplied the area of each land unit that simulated by Markov-PLUS model with land use carbon emissions coefficient of the corresponding land use type respectively to obtain the carbon emissions of each land unit. Finally, ArcGIS software was applied to summarize carbon emissions of land units to ULUCM units, and carbon emissions on ULUCM units were calculated.

3.2. Simulating land use carbon sequestration pattern

LANDIS model was applied to define the ecological carbon sequestration potential level based on the vegetation growth and dominant tree species in the landscape patch. In the process of community growth and succession in the landscape patch, the richer the species diversity, the higher the distribution uniformity and the larger the distribution space of the tree community, the greater its carbon sequestration potential.

The classification for site types. To run LANDIS model, the regions should be divided into effective and ineffective regions. Ineffective regions were industrial and mining land, transportation and other construction land, water and other non-forest land, while effective regions were divided into 8 site types according to local elevation, slope, aspect of slope, and tree growth habits (Tab.3).

Table.3 Classification criteria for site types

Serial number	Slope	Aspect	Altitude	Area (km^2)
S0	⩽25°	Sunny slope	⩽150	357.65
S1	⩽25°	Sunny slope	>150	51.07
S2	⩽25°	Shade slope	⩽150	402.12
S3	⩽25°	Shade slope	>150	153.59
S4	＞25°	Sunny slope	⩽150	18.41
S5	＞25°	Sunny slope	>150	28.27

Serial number	Slope	Aspect	Altitude	Area (km^2)
S6	＞25°	Shade slope	⩽150	132.11
S7	＞25°	Shade slope	>150	141.67
S8		Non-forest		1578.36

Tree species parameter setting. Based on the forest characteristics of tree species, we selected the dominant species in the vegetation community as the model tree species. Dongguan's forest vegetation type is mainly the South Asian monsoon evergreen broad-leaved forest. Therefore, camphor tree, masson pine, China fir, moso bamboo, tung tree and schima root-bark were selected as simulation tree species. In addition, based on field investigation and expert consultation, we set the life history characteristic parameters of the above tree species as simulation parameters (Tab.4).

Table.4 Life history characteristic parameters of main tree species

Tree species	Life(age)	Maturation age	Shade tolerance	Fire resistance	Effective travel distance(m)	Maximum propagation distance(m)	Germination probability	Germination age
camphor tree	200	30	5	1	63	200	0.66	6
Masson pine	300	10	4	1	250	1000	0	0
China fir	200	10	5	1	200	750	0.2	3
Moso bamboo	60	10	2	1	250	800	0.3	2
Tung tree	260	40	4	4	100	500	0.5	4
Schima root-bark	300	20	5	5	50	200	0.68	5

Simulation of land use carbon sequestration pattern. Though the LANDIS model can be applied to predict the future vegetation type and distribution, it is difficult to accurately estimate the absolute amount of land use carbon sequestration. As previously mentioned, the amount of carbon sequestration is closely related to the area, shape and uniformity of vegetation. Therefore, we proposed carbon sequestration potential (CSP) from the above aspects to represent the relative value of carbon sequestration on ULUCM units, and to predict the future pattern of land use carbon sequestration. CSP on ULUCM units was calculated as follows:

$$CSP_{ULUCM(i)} = Std_{PLAND(i)} \bullet \omega_a + Std_{FRAC\_MN(i)} \bullet \omega_b + Std_{AI(i)} \bullet \omega_c \quad (4)$$

where $CSP_{ULUCM(i)}$ represents the carbon sequestration potential on ULUCM unit *i*; $Std_{PLAND(i)}$ represents the standardized value for the proportion of vegetation area on ULUCM unit *i* to the total vegetation area (PLAND). $Std_{FRAC\_MN(i)}$ represents the standardized value for the mean fractal dimension index of vegetation patches on ULUCM unit *i* (FRAN_MN); $Std_{AI(i)}$ represents the aggregation index of vegetation patches on ULUCM unit *i* (AI); ω_a, ω_b, and ω_c represents the weight of $Std_{PLAND(i)}$, $Std_{FRAC\_MN(i)}$, and $Std_{AI(i)}$, they were set as 0.4, 0.3, and 0.3, respectively. PLAND, FRAC_MN, and AI were calculated on Fragstats 4.2 platform.

3.3. Identifying the weak areas of ULUCM

The carbon metabolism capacity on ULUCM units were calculated according to:

$$(ULUCM)_i = (CE)_i / (CS)_i \quad (5)$$

where $(ULUCM)_i$, $(CE)_i$, and $(CS)_i$ represent the capacity of ULUCM, carbon emissions, and carbon sequestration on ULUCM unit *i*, respectively. Natural breakpoint classification method was applied to divide ULUCM's capacity into 4 levels (strong area, sub-strong area, sub-weak area, and weak area).

4. Results

4.1. Carbon emissions from energy consumption

As Fig.3a, 3b, and 3c shown, the total carbon emissions in 2030 were 71.2 Mt, 51 Mt, and 43.8 Mt in baseline, carbon-reduction, and high-limit scenario, respectively. In baseline scenario, Dongguan's carbon emissions of energy consumption increase to 71.2 Mt in 2030. In carbon-reduction scenario, because of energy efficiency optimization, electrification optimization and other measures, the carbon emissions rise slowly to 51.0 Mt in 2030, 28% lower than baseline scenario. In high-limit scenario, due to the strict implementation of emissions reduction measures, the terminal energy consumption continues to decline, and the carbon emissions in 2030 are only 43.8Mt, 38% lower than baseline scenario. As the baseline scenario takes the current policy measures and technology level as the development direction, Dongguan's final energy consumption will continue to rise, and it is difficult to

achieve the carbon peak in 2030. In carbon-reduction scenario, measures such as industrial structure optimization, energy efficiency improvement, electrification, and promotion of clean electricity are added on the basis of the baseline scenario, so the terminal energy consumption is expected to rise slowly and carbon peak is expected to be achieved in 2030. In high-limit scenario, the emissions reduction measures are further strengthened, and the terminal energy consumption can be effectively reduced before and after 2025, and the carbon peak goal can be achieved in advance.

In the carbon emissions structure, the LEAP model is broken down into four major industries, namely construction, transportation, industry, and agriculture and forestry. Overall, the industrial sector accounts for the largest share of carbon emissions. In all three scenarios, industrial carbon emissions account for more than 50% of total carbon emissions. In baseline scenario, industrial carbon emissions in 2030 can reach 39.25 Mt, and the carbon-reduction scenario and high-limit scenario can reach 28.44 Mt and 25.58 Mt, respectively. In the transportation industry, due to the developed warehousing and logistics industry in Dongguan, transportation energy consumption is large. Even if emissions reduction measures are implemented, the transportation carbon emissions in the baseline scenario still increase significantly. However, the traffic carbon emissions of carbon-reduction scenario and high-limit scenario can be effectively controlled under emissions reduction measures, and the growth is slow. Among them, the transport carbon emissions in carbon-reduction scenario will increase to 13.4 Mt in 2030, and in high-limit scenario will increase to 9.7 Mt in 2030. Compared with baseline scenario, carbon-reduction and high-limit scenario are more effective in energy conservation and emissions reduction measures, and the carbon emissions of industries can be effectively controlled.

As Fig.3d, Fig.3e shown, in carbon-reduction scenario, the biggest contribution is the improvement of energy efficiency, which will reduce carbon emissions by 63.21 Mt. This is followed by electrification, which can reduce carbon emissions by 37.10 Mt. In high-limit scenario, the most effective carbon reduction measures are also the improvement of energy efficiency and electrification. In conclude, measures of energy efficiency improvement and electrification have a significant effect on reducing carbon emissions in the short term.

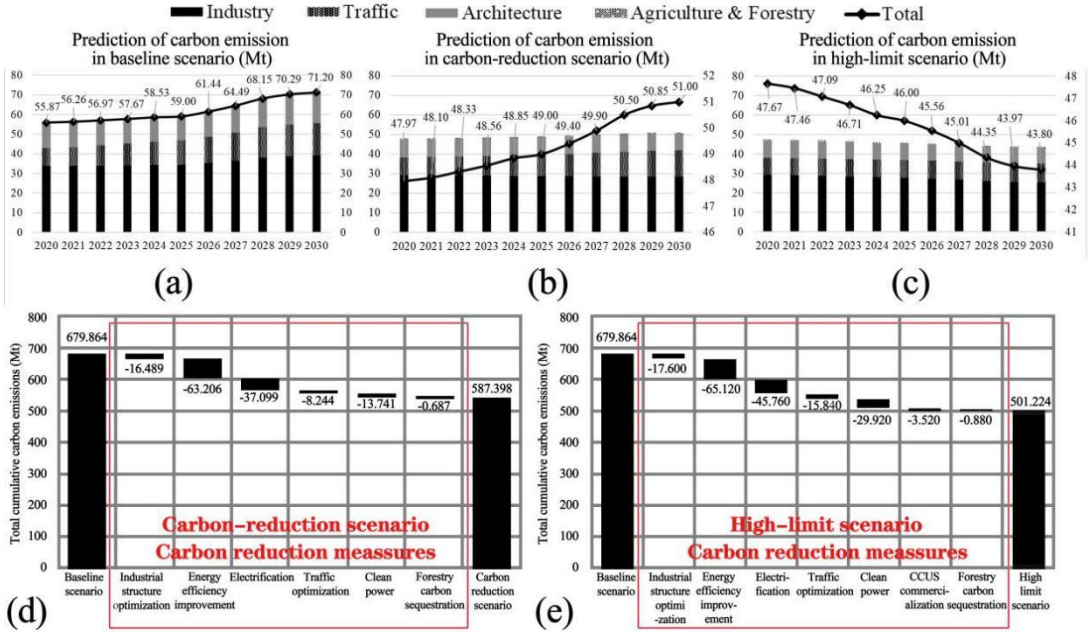

Figure.3 Total carbon emissions of different industries under different scenarios (a, b, c) and contribution of different measures to carbon reduction (d, e)

4.2. Carbon emissions on ULUCM units

Fig.4a, Fig.4b, and Tab.5 depict the the land use structure in 2030 simulated with Markov-PLUS model. The expansion of industry and architecture land will occupy part of agricultural & forest land, green space, and water area. The expansion mainly occurs in the dam area, river valley and low-lying area, although the expansion area is small, the scope is small, but the expansion ratio is large. Accordingly, the land use carbon emissions coefficient of agricultural & forest land, industry land, architecture land, and traffic land in different scenario was calculated. Other land-use types are not for living and production, and the total area is generally decreasing, their carbon emissions were assumed to be zero. Finally, the land use carbon emissions pattern of three scenarios were mapped as Fig.4c, 4d, and 4e. On

the whole, high carbon emissions regions are mainly concentrated in the central, southwest and southeast of Dongguan. These regions are characterized by high energy consumption and carbon emissions. Baseline scenario has the largest area of high carbon emissions regions, followed by the carbon-reduction and high-limit scenario.

In carbon-reduction scenario, the proportion of non-fossil energy consumption in the manufacturing industry has dropped to 70%, which basically meets the requirements of the "Dongguan Energy 14th Five-Year Plan" (by 2030, the proportion of natural gas consumption of Dongguan should reach 39%, and the proportion of primary electricity and other energy consumption should reach 36%). In addition, under the premise of increasing forestry carbon sink, the forest coverage rate of Dongguan would reach 42% by 2030, exceeding the target of 37% coverage rate in "Dongguan Ecological Environment 14th Five-Year Plan". Furthermore, if measures of clean power are further adopted, the proportion of non-fossil energy power generation in Dongguan would reach 70% in 2030, which meets the requirements of 49% non-fossil energy power generation in "Guangdong 14th Five-Year Energy Plan".

Finally, the distribution of high carbon emissions regions did not conflict with the forest parks and ecological protection areas in "Dongguan 14th Five-Year Ecological Environment Plan". The high carbon emissions regions could be restricted by constructing ecological corridor, setting up carbon emissions expansion control belt and repairing ecological base. Comparatively speaking, the high-limit scenario is the idealized scenario. Although the land use carbon emissions pattern tends to be reasonable, measures such as electrification, traffic operation optimization, and clean electricity temporarily lack conditions for implementation.

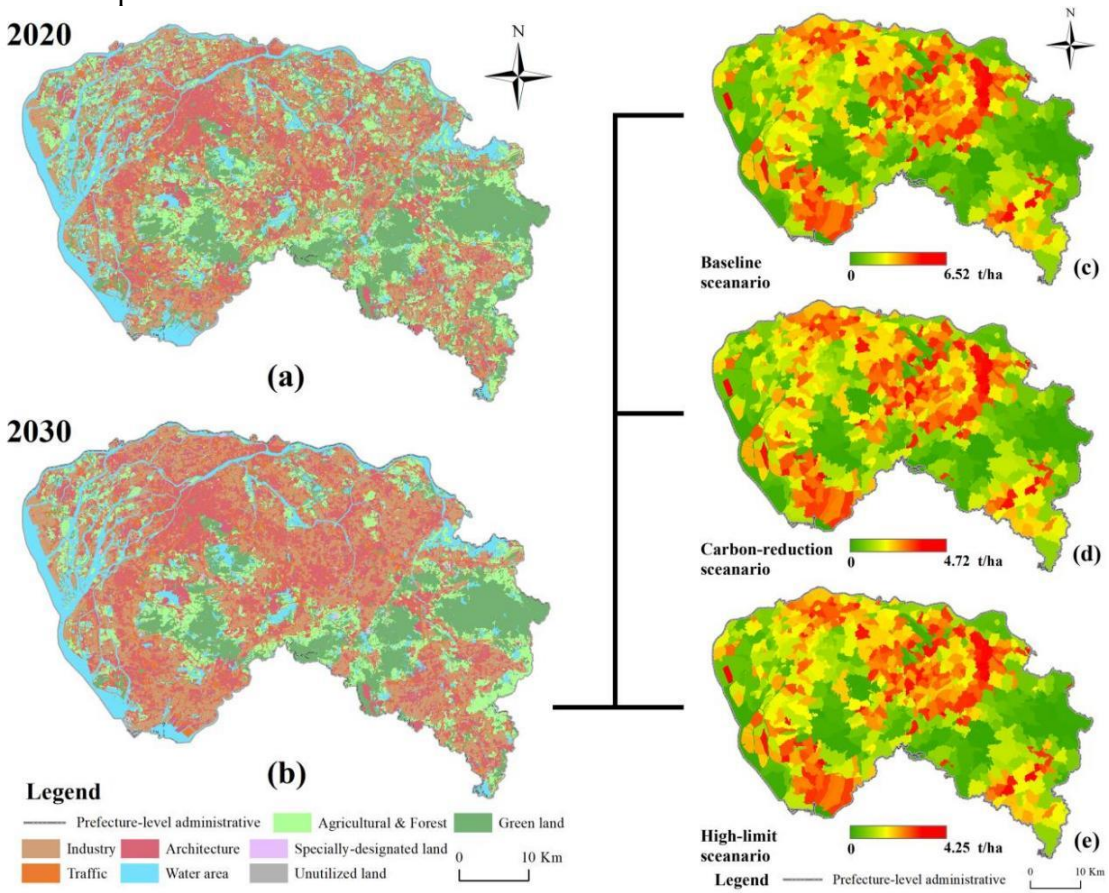

Figure.4 Land use pattern (a, b) and land use carbon emissions pattern (c, d, e)

Table.5 Structural change and carbon emissions coefficient of different land types

Land type	Area			Land use carbon emissions coefficient (t/ha)		
	In 2020(ha)	In 2030(ha)	2030-2020(ha)	Baseline	Carbon-reduction	High-limit
Agricultural & Forest	40551.48	29942.02	-10609.46	0.4065	0.3393	0.2234
Green space	50013.98	36505.67	-13508.31	-	-	-
Industry	44812.7	60210.3	15397.6	6.5190	4.7244	4.2481
Architecture	45377.26	55735.45	10358.19	2.5659	1.4581	1.4097
Specially-designated	1247.1	1464.08	216.98	-	-	-
Traffic	26587.16	30505.6	3918.44	5.3862	4.3959	3.1784
Water area	36003.06	31595.57	-4407.49	-	-	-

Unutilized land	1418.76	52.81	-1365.95	-	-	-

4.3. Carbon sequestration on ULUCM units

As Fig.5a shown, Due to the restriction of construction land, there is little space for the natural expansion of vegetation in Dongguan's. The vegetation growth in the eastern and southern arboreal communities was the best, and the vegetation distribution area was the widest. The total vegetation area is 87209.71 ha, which account for 35.45% of Dongguan's administrative area. According to the simulation results, though the total amount of camphor trees and masson pines are roughly equivalent, their distribution characteristics are significantly different. Through analyzing the distribution of tree species and the land use pattern in 2030, it was found that the total vegetation area reached 24250.56 ha in industrial land, architecture land, specially-designated land, and traffic land, which accounted for 27.81% of the total vegetation area. Therefore, even the construction land has sufficient conditions for vegetation growth. For Dongguan, in order to enhance the overall carbon metabolism capacity, in addition to expanding a large area of green space, enhancing the carbon sink capacity of non-green space is also a long-term way.

As Fig.5b shown, the maximum, minimum, mean, and median CSP values are 92.98, 0, 43.84, and 44.69. Only three ULUCM units have a CSP value greater than 70. However, there are 492 ULUCM units with CSP values between 40 and 50. It can be seen that the overall land use carbon sequestration capacity of high-density city is relatively limited in terms of the current rule of vegetation growth. The enhancement of UCM capacity has to rely more on far-sighted polices and planning tools. In addition, the most correlated variable with CSP value is AI. The focus of future green space planning should be to connect the existing green space, not only to expand the area of vegetation. FRAC of vegetation is also a very important variable, however, it is difficult to have room for improvement due to the restriction of the construction land pattern. Thus, in non-green space, the focus of enhancing carbon sequestration should be to optimize the shape and improve the concentration of vegetation.

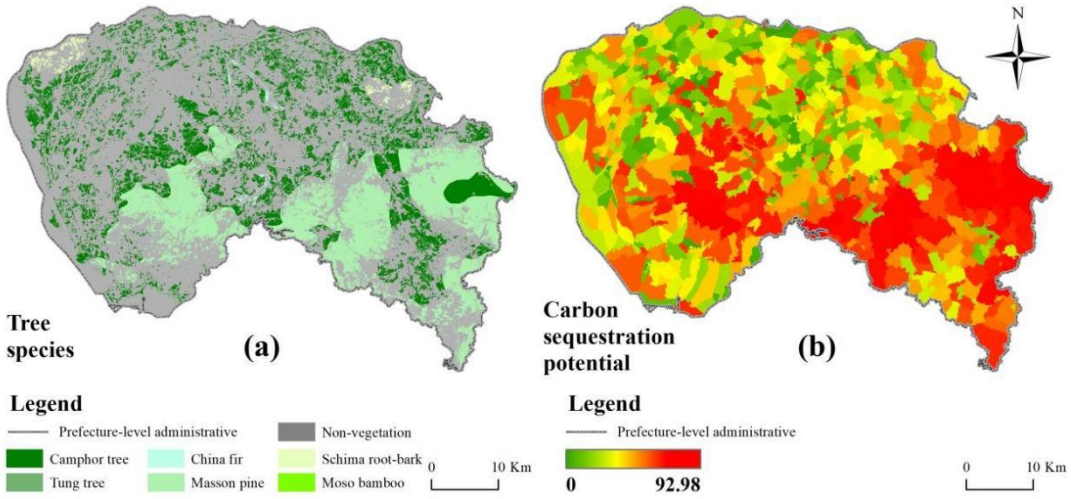

Figure.5 Simulation of tree species (a) and carbon sequestration on ULUCM units (b)

4.4. Identification of weak areas in ULUCM pattern

As Fig 6a, 6b, and 6c shown, the distribution curve of CE/CS in baseline scenario and high-limit scenario is steep, which means that the difference of CE/CS between various ULUCM units is small. In addition, the absolute value of CE/CS in the baseline scenario is higher, while in the high-limit scenario is smaller. The distribution curve of CE/CS in carbon-reduction scenario is slightly flat, which means that the difference of CE/CS between various ULUCM units is more obvious.

As Fig 6d, 6e, and 6f shown, because of the difference in total carbon emissions, the ULUCM units in Dongguan showed different patterns in three scenarios after they were dividing into 4 categories. After calculation, there were 47, 70, and 65 ULUCM units were identified as weak area in in baseline scenario, carbon-reduction scenario, and high-limit scenario, respectively. The covering area were 8088 ha, 13177 ha, and 12717 ha, respectively. The average CE/CS was 0.14, 0.095, and 0.083, respectively.

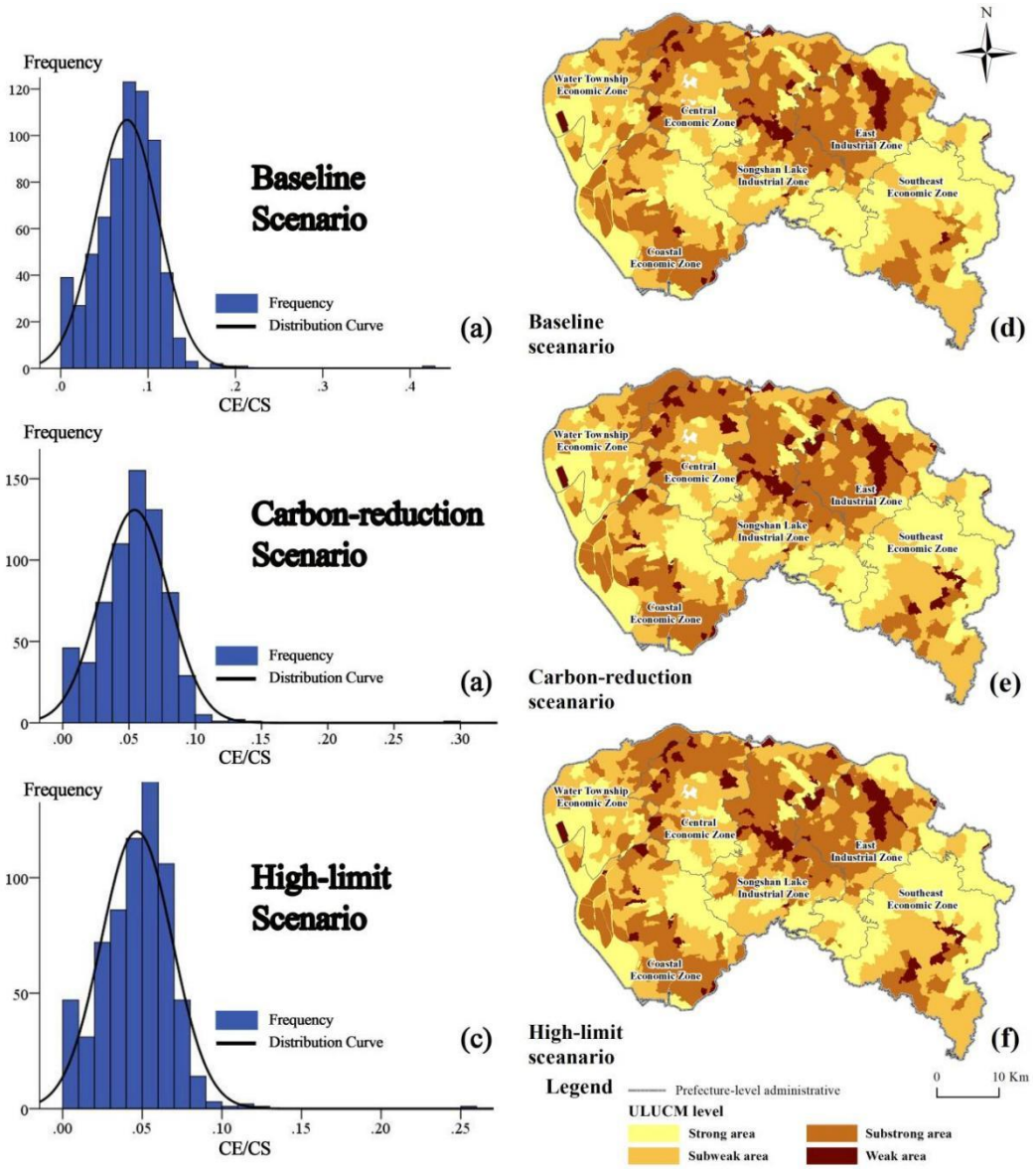

Figure.6 Frequency (a,b,c) and distribution (d,e,f) of CECS in three scenarios

On the whole, due to the large growth rate of industrial land, the total carbon emissions of energy consumption in Dongguan will be maintained at a high level in the future. At the same time, the space for vegetation growth is insufficient. If it is left to develop freely, the capacity of ULUCM will become increasingly weak. Looking forward to 2030, the emission-reduction scenario requires more specific policies to curb the adverse effects of weak carbon metabolism areas.

5. Discussions

5.1. Advantages and disadvantages of the study framework

Green space planning is the main measure to enhance the capacity of ULUCM. When planning urban green space, planners usually investigate the current conditions in detail to summarize the current patterns of carbon flow in cities. This is intended to identify the path for minimizing the disturbance to the stability of UCM system due to economic development and land expansion [11]. After distinguishing the weak area of ULUCM, the green space can be purposefully reconstructed to increase the carbon metabolism capacity and ecological benefit. However, green space planning is a relatively passive and backward means of administrative management. Although it can solve the problems existing in the past and current UCM system, it is difficult to take into account the impact of future economic and industrial development.

The prediction for ULUCM pattern was an important step to understanding UCM comprehensively, as well as a scientific reference for designing targeted measures to reduce carbon emissions and increase carbon sequestration in planning high-density city area [18-20]. They mainly focused on the ULUCM pattern generated by LUCC pattern. However, the prediction of land use carbon emissions at urban scale may not consistent with carbon emissions prediction of energy consumption at

regional scale. The influence of regional carbon reduction policies on ULUCM pattern is uncertain. By analyzing a typical case of a high-density urbanized area, this study conducted a complex ecological framework aimed at identifying the weak area of future ULUCM, which belongs to the applied study of simulating ULUCM pattern. This framework combines the principles of LEAP, Markov-Plus, and LANDIS models, which serves the following purposes: 1) To spatialize the carbon emissions from energy consumption predicted at regional scale. 2) To evaluate the carrying capacity of urban vegetation habitats for carbon emissions reduction strategies under different scenarios. 3) To identify the weak areas of ULUCM pattern in high-density cities, and help administrators locate the carbon sequestration nodes under specific scenarios.

Therefore, compared with previous studies, the significance of this study framework is that the carbon emissions of urban energy consumption and land use expansion are taken into account in simulating the UCM pattern. The effect of urban carbon reduction policies can be clearly spatialized. The green space planning formed according to the simulated pattern can also reduce certain uncertainties.

5.2. Rationality for the spatial pattern of weak areas

The significance of this study's methodology is that it simulates the UCM pattern while also accounting for the carbon emissions caused by urban energy consumption and land use expansion. This is consistent with the findings of most studies [11]. In the calculation process, we assumed that the carbon emissions of energy consumption mainly come from four land use types of agricultural & forest land, industry land, architecture land, and traffic land. ULUCM units that with larger area of the above four land use types should have weaker capacity of carbon metabolism. However, this law is not absolutely true. As Fig.7 shown, taking carbon-reduction scenario as example, we divided PLAND, FRAC, and AI into four categories of strong, sub-strong, sub-weak, and weak, to analyze the relationship between CE/CS and CSP on ULUCM units. We found that ULCUM units with strong PLAND can also be identified as areas with weak CE/CR (Fig. 7a, histogram ④); those with sub-weak PLAND could also be identified as areas with sub-strong CE/CR (Fig. 7a, histogram ②); those with sub-strong FRAC could also be identified as areas with sub-weak CE/CR (Fig. 7b, histogram ③); those with sub-strong AI could also be identified as areas with sub-weak CE/CR (Fig. 7c, histogram ③). It can be inferred that vegetation coverage is not a decisive factor for carbon metabolism. The reason is that the poor shape and concentration of vegetation on these ULUCM units makes their CSP at a low level. Even ULUCM units with high carbon emissions, if the vegetation on them has better shape and concentration, their carbon metabolism capacity will improve.

Therefore, for the green space planning of high-density cities, it is necessary to focus on the optimization of the shape and concentration conditions of existing vegetation, rather than increasing the coverage area of vegetation. These results were in line with those of Wang et al. (2022), who took into account the factors influencing vegetation's capacity to store carbon in the terrestrial environment [20].

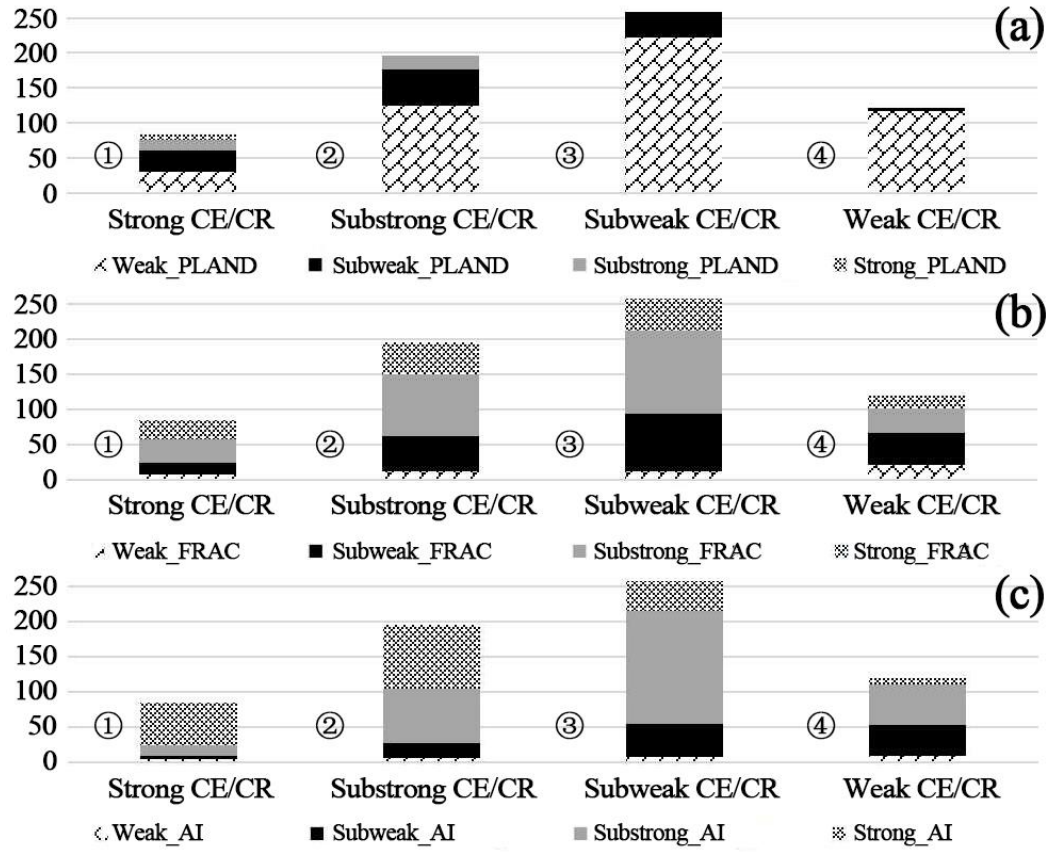

Figure.7 The relationship between CECR and PLAND(a), FRAC(b), AI(c)

5.3. Practical applications for green space planning

After identifying the weak areas of urban carbon metabolism, targeted methods can be adopted to reconstruct the existing green space. Here, according to the enlightenment from the result analysis, we selected the ULUCM pattern in carbon-reduction scenario as the object, and tried to form an optimization path and strategy.

As Fig.8 shown, first, the weak areas of ULUCM were regarded as nodes for increasing carbon sequestration. Then, oxygen-source green space, carbon-source green space, and near-source green space of the study area were delimited according to the distribution of nodes and vegetation pattern simulated by LANDIS model. Among, oxygen-source green space is located upwind of the region and can provide the functions of carbon fixation, oxygen release and dust retention. It includes the green space between Coastal Economic Zone and Songshan Lake Industrial Zone, in the south of Songshan Lake Industrial Zone, and in the northeast of Southeast Economic Zone. Carbon-source green space is located downwind of the region and can effectively absorb urban carbon emissions. It includes the green space in the north of Water Township Economic Zone, in the north of Songshan Lake Industrial Zone, and in the north of East Industrial Zone. Near-source green space is located within the built-up area with local ecological function. Second, nodes were connected with similar spatial distances to form carbon emissions limit regions, which served as a barrier for carbon emissions from weak areas. Finally, various types of ecological corridors were delineated to connect the carbon emissions limit regions, so as green spaces can effectively metabolize carbon emissions from weak areas.

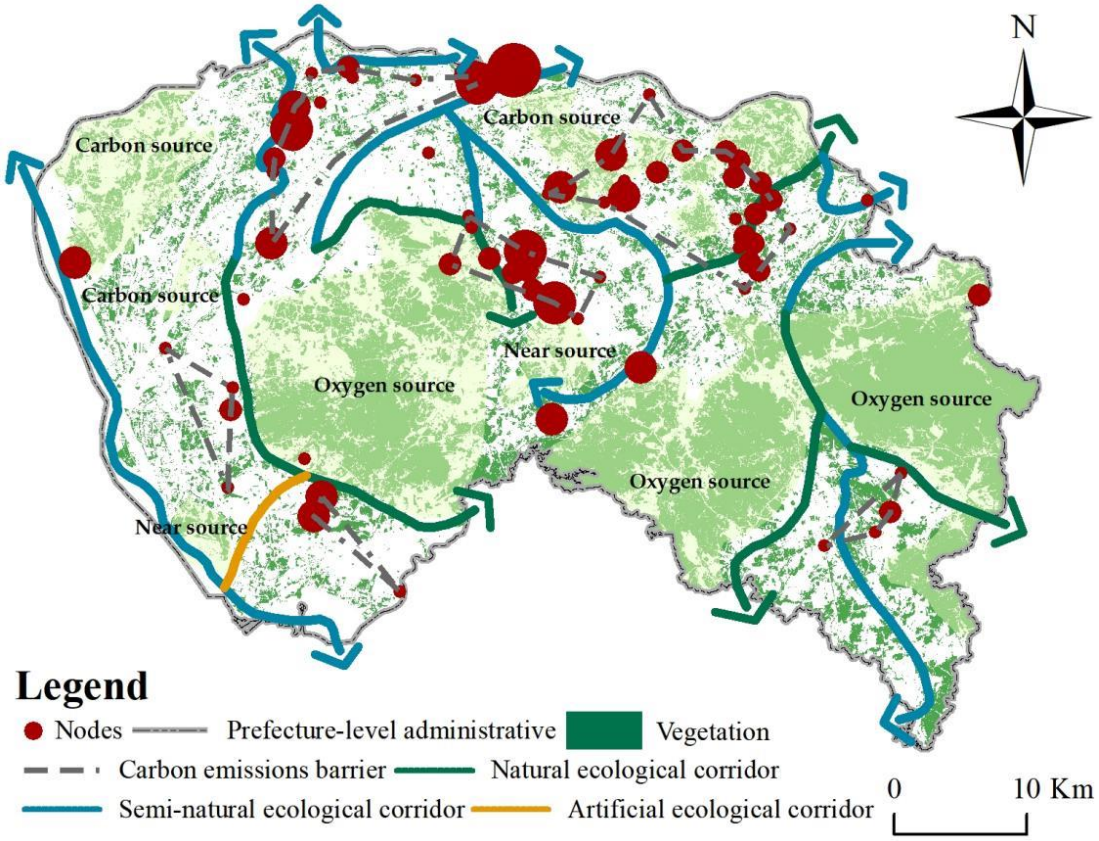

Figure.8 The optimization of the green spaces based on the study results

5.4. Limitations and suggestions for future research

The study has some issues that need to be addressed in further. First, the study may have been biased because the spatial difference of carbon emissions coefficient was ignored in the process of simulating the land use carbon emissions pattern. The future land use carbon emissions coefficient in the study was calculated according to the total future carbon emissions from energy consumption and future land use area. In this way, the carbon emissions coefficient of each land patch in the region is the same. In fact, even in high-density cities, there are regional differences in carbon emissions. Although the difference may be small, it cannot be easily dismissed. This also makes the study framework may only be used in high-density cities currently. Therefore, how to accurately predict the difference of carbon emissions coefficient in different regions or even different land patches in the future is one of the key research points.

Second, a comprehensive index was constructed using PLAND, FRAC and AI to represent the carbon sequestration potential of vegetation simulated by LANDIS model. The capability for sequestering carbon is, however, very strongly correlated with the kind and development of plants. According to the current simulation results, the proportion of camphor and masson pine is large, and the proportion of other tree species is small, so the simulation results can not be considered accurate. In addition, the study did not take into account the growth of vegetation in different regions. These also make the calculation of ULUCM capacity biased. Therefore, further research will be conducted on techniques to accurately simulate future tree species patterns and improve the calculation accuracy of carbon sequestration potential.

Third, the ULUCM capacity was calculated by using the possible carbon emissions and carbon sequestration. This effectively assumed that ULUCM units were static and enclosed space. Previous studies have also shown that UCM is a dynamic process, which should be studied by using ecological network.

6. Conclusions

Using Dongguan as a research case, this study proposed a complex ecological framework to identify the weak areas of future ULUCM pattern for high-density region facing a situation with high and increasing energy consumption. Through overlapping the spatial pattern of land use carbon emissions and carbon sequestration simulated by LEAP, Markov-Plus, and LANDIS mode, the future weak areas of carbon metabolism were clearly indicated. The novelty of this study is that it combines the prediction

of carbon emissions from energy consumption at regional scale, of land use carbon emissions pattern at urban scale, which expands the technology for simulating land use carbon metabolism pattern. With the help of these findings, urban planners will be better able to comprehend how patterns of carbon metabolism alter depending on the type of carbon emissions strategy being used. As a result, this article will serve as a foundation to plan and control carbon emissions in high-density cities that are similar to Dongguan in international communities.

Data Sharing Statement: The data that support the findings of this study are available from the corresponding author upon reasonable request.

Competing Interests: The authors have no relevant financial or non-financial interests to disclose.

Acknowledgements: This study was supported by the Project supported by the Key Laboratory of Natural Resources Monitoring in Tropical and Subtropical Area of South China, Ministry of Natural Resources (NO. 2023NRMK01), the Guangzhou Science and Technology Planning Project (NO. 202102021023), the Natural Science Foundation of Guangdong Province (NO. 2021A1515110531, 2021A1515110971), the National Natural Science Foundation Project (NO. 42071356), and the Science and technology project of Natural Resources Department of Guangdong Province (NO. GDZRZYKJ2024004).

Author Contributions: Conceptualization: Zongliang Lu, Yilun Liu, Liying Yang; Data curation: Zongliang Lu, Lu Yi; Formal analysis: Zongliang Lu; Methodology: Zongliang Lu, Lu Yi; Project administration: Liying Yang, Yilun Liu; Investigation: Xiaobing Zhang; Resources: Zongliang Lu, Lu Yi; Software: Zongliang Lu, Lu Yi, Xiaobing Zhang; Supervision: Liying Yang, Yilun Liu; Visualization: Xiaobing Zhang; Validation: Zongliang Lu, Xiaobing Zhang; Funding acquisition: Zongliang Lu, Yilun Liu; Writing – original draft: Zongliang Lu, Xiaobing Zhang; Writing – review & editing: Liying Yang, Yilun Liu.

Reference

[1] Grimm, N.B., Faeth, S.H., Golubiewski, N.E., Redman, C.L., et al. Global change and the ecology of cities[J]. *Science, 319*(2008), 5864, pp.756-760. DOI: 10.1126/science.1150195

[2] Zhang Y, Linlin X, Weining X. Analyzing spatial patterns of urban carbon metabolism: A case study in Beijing, China. *Landscape and Urban Planning, 130*(2014), pp.184-200. DOI: 10.1016/j.landurbplan.2014.05.006

[3] Chen Q, Su M, Meng F, et al. Analysis of urban carbon metabolism characteristics based on provincial input-output tables. *Journal of Environmental Management, 265*(2020), 110561. DOI: 10.1016/j.jenvman.2020.110561

[4] Baccini, P. Understanding regional metabolism for a sustainable development of urban systems. *Environmental Science and Pollution Research, 3*(1996), 2, pp.108-111. DOI: 10.1007/BF02985503

[5] Xia L, Zhang Y, Wu Q, et al. Analysis of the ecological relationships of urban carbon metabolism based on the eight nodes spatial network model. *Journal of Cleaner Production, 140*(2017), pp.1644-1651. DOI: 10.1016/j.jclepro.2017.09.077

[6] Cai C, Fan M, Yao J, et al. Spatial-temporal characteristics of carbon emissions corrected by socio-economic driving factors under land use changes in Sichuan Province, southwestern China. *Ecological Informatics, 77*(2023), 102164. DOI: 10.1016/j.ecoinf.2023.102164

[7] Cai B, Zhang L, Xia C, et al. A new model for China's CO2 emission pathway using the top-down and bottom-up approaches. *Chinese Journal of Population, Resources and Environment, 19*(2021), 4, pp.291-294. DOI: doi.org/10.1016/j.cjpre.2022.01.001

[8] Unnewehr J F, Weidlich A, Gfüllner L, et al. Open-data based carbon emission intensity signals for electricity generation in European countries – top down vs. bottom up approach. *Cleaner Energy Systems, 3*(2022), 4, 100018. DOI: 10.48550/arXiv.2110.07999

[9] Yang J, Deng Z, Guo S, et al. Development of bottom-up model to estimate dynamic carbon emission for city-scale buildings. *Applied Energy, 331*(2023), 120410. DOI: doi.org/10.1016/j.apenergy.2022.12041

[10] Zhang C, Luo H. Research on carbon emission peak prediction and path of China's public buildings: Scenario analysis based on LEAP model[J]. *Energy and Buildings, 289*(2023), 113053. DOI: 10.1016/j.enbuild.2023.113053

[11] Zhang Y, Wu Q, Fath B D. Review of spatial analysis of urban carbon metabolism. *Ecological Modelling, 371*(2018), pp.18-24. DOI: 10.1016/j.ecolmodel.2018.01.005

[12] Xia C, Li Y, Xu T, et al. Analyzing spatial patterns of urban carbon metabolism and its response to change of urban size: A case of the Yangtze River Delta, China. *Ecological Indicators, 104*(2019), pp.615-625. DOI: 10.1016/j.ecolmodel.2017.03.002

[13] Zhang F, Xu N, Wang C, et al. Effects of land use and land cover change on carbon sequestration and adaptive management in Shanghai, China. *Physics and Chemistry of the Earth, 120*(2020), 102948. DOI: doi.org/10.1016/j.pce.2020.102948

[14] Cui X, Li S, Gao F. Examining spatial carbon metabolism: Features, future simulation, and land-based mitigation. *Ecological Modelling, 438*(2020), *109325.* DOI: doi.org/10.1016/j.ecolmodel.2020.109325

[15] Chrysoulakis N, Lopes M, San José R, et al. Sustainable urban metabolism as a link between bio-physical sciences and urban planning: The BRIDGE project. *Landscape and Urban Planning, 112*(2013), pp.100-117. DOI: 10.1016/j.landurbplan.2012.12.005

[16] Jing Z, Zhuang S, Chuyu X, et al. Ecosystem services assessment based on land use simulation: A case study in the Heihe River Basin, China. *Ecological Indicators, 143*(2022), 109402. DOI: doi.org/10.1016/j.ecolind.2022.109402

[17] Zhao N Z, Liu Y, Cao G F, et al. Forecasting China's GDP at the pixel level using nighttime lights time series and population images. *GISCIENCE & REMOTE SENSING, 54*(2017), 3, pp:407-425. DOI: 10.1080/15481603.2016.1276705

[18] Chen S Q, Chen B. Determining carbon metabolism in urban areas though network environ theory. *Procedia Environmental Sciences, 13*(2012), pp:2246-2255. DOI: doi.org/10.1016/j.proenv.2012.01.213

[19] Xia L, Liu Y, Wang X, et al. Spatial analysis of the ecological relationships of urban carbon metabolism based on an 18 nodes network model. *Journal of Cleaner Production, 170*(2018), pp:61-69. DOI: 10.1016/j.jclepro.2017.09.077

[20] Wang A, Kafy A A, Rahaman Z A, et al. Investigating drivers impacting vegetation carbon sequestration capacity on the terrestrial environment in 127 Chinese cities. *Environmental and Sustainability Indicators, 16*(2022), 100213. DOI: doi.org/10.1016/j.indic.2022.100213